An Improved Method for Transforming GPS/INS Attitude to National Map Projection Frame

Xiang Shen (沈翔), Yongjun Zhang (张永军), Xiao Lu (鲁潇), Qian Xie (谢谦), and Qingquan Li (李清泉)

***Abstract*—Global Positioning System/Inertial Navigation System (GPS/INS) integrated navigation systems play a very important role in modern photogrammetry and laser scanning by virtue of their capability of direct measurement of high-precision position and attitude data in the WGS 84 datum. In practice, as georeferencing is often conducted in national coordinates, there is a need to transform GPS/INS data to the required national map projection frame first. This letter presents an improved coordinate-transformation-based method for the GPS/INS attitude transformation by taking the datum scale distortion and the length distortion into account. Experimental results show that the transformation errors of our improved method are on the order of magnitude of $1 \times 10^{-5^\circ}$, which can be safely ignored in aerial photogrammetric processing, whereas the maximum error of the previous coordinate-transformation-based method can be up to several 0.001°.**

***Index Terms*—Global Positioning System/Inertial Navigation System (GPS/INS), orientation, photogrammetry, transformation.**

I. Introduction

SINCE the end of the last century, airborne imaging sensors have been increasingly equipped with Global Positioning System/Inertial Navigation System (GPS/INS) integrated navigation systems (a.k.a. position and orientation systems, (POS) in the photogrammetric community), which benefit from their capability to directly obtain high-precision position and attitude information of sensor platforms [1], [2]. Raw GPS/INS data are measured and processed in the WGS 84 datum, and accordingly, the outputted position and attitude data are typically provided in some frames related to the WGS 84 datum directly. On the other hand, aerial photogrammetry and light detection and ranging (LiDAR) data products (e.g., digital surface models, digital terrain models, and orthophotos) are commonly required in national coordinates, and it is accordingly more convenient and customary to use the national map projection frame for georeferencing and other subsequent processing operations [3], [4]. Therefore, in practice, GPS/INS position and attitude data are usually required to be transformed to the desired national map projection frame first [5].

Currently, the transformation formulas of GPS/INS position data to national coordinates can be easily found in many geospatial references [6]. The attitude transformation problem, on the other hand, is less well understood. Different from previous studies [3], [5], Zhao *et al.* have recently proposed an alternative GPS/INS attitude transformation algorithm that uses coordinate transformation results to indirectly solve the attitude matrix in the national map projection frame [7]. However, according to our test results, the performance of their method has not been fully optimized. In this letter, we will present an improved algorithm and show that the transformation errors of the method of Zhao *et al.* can be greatly reduced by considering the georeferencing distortions in national coordinates.

The remainder of this letter is organized as follows. Section II provides some background material on the GPS/INS attitude transformation problem. Then, in Section III, we analyze the method of Zhao *et al.* and develop our improved algorithm. In the last two sections, we present comparative experimental results and conclude this letter.

II. Background

A. Reference Frames

For establishing the transformation relations between different reference frames, a first and fundamental issue is to clearly define all involved frames [8]. The reference frames used in this letter and their detailed definitions are listed in the following.

1) Sensor frame (s-frame). The coordinate origin is the optical center of the sensor (e.g., a frame camera or LiDAR). The X- and Y-axes typically point backward along and right of the flight direction, respectively; and the Z-axis points upward.
2) Body frame (b-frame). The coordinate origin usually chooses the inertial measurement unit (IMU) center. The X- and Y-axes point forward along and right of the flight direction, respectively; and the Z-axis points downward.

Manuscript received August 16, 2014; revised December 20, 2014; accepted January 21, 2015. This work was supported in part by the National Natural Science Foundation of China under Grant 41322010 and Grant 41171292.

X. Shen is with the Shenzhen Key Laboratory of Spatial Smart Sensing and Services; the Key Laboratory for Geo-Environment Monitoring of Coastal Zone of the National Administration of Surveying, Mapping and Geoinformation; and the College of Information Engineering, Shenzhen University, Shenzhen 518060, China, and also with the School of Remote Sensing and Information Engineering, Wuhan University, Wuhan 430079, China.

Y. Zhang is with the School of Remote Sensing and Information Engineering, Wuhan University, Wuhan 430079, China (e-mail: zhangyj@whu.edu.cn).

X. Lu is with United Remote Sensing Technology Company, Ltd., Beijing 100037, China.

Q. Xie is with The Second Institute of Photogrammetry and Remote Sensing, National Administration of Surveying, Mapping and Geoinformation, Harbin 150081, China, and also with Heilongjiang Longfei Aerial Photography Company, Ltd., Harbin 150081, China.

Q. Li is with the Shenzhen Key Laboratory of Spatial Smart Sensing and Services and the Key Laboratory for Geo-Environment Monitoring of Coastal Zone of the National Administration of Surveying, Mapping and Geoinformation, Shenzhen University, Shenzhen 518060, China.

Color versions of one or more of the figures in this paper are available online at http://ieeexplore.ieee.org.

Digital Object Identifier 10.1109/LGRS.2015.2396518

3) Navigation frame (n-frame). This frame is a local level frame of the WGS 84 datum ellipsoid. The coordinate origin is the same as the b-frame, and the axis directions follow the north–east–down convention.
4) Earth-centered Earth-fixed frame (e-frame). It refers specifically to the WGS 84 reference frame.
5) Eccentric Earth-fixed frame (e′-frame). This Earth-fixed frame is defined by the national datum. Its coordinate origin is at the center of the national datum, which usually slightly deviates from that of the WGS 84 datum.
6) National map projection frame (p-frame). This frame typically uses a conformal map projection.

B. Georeferencing Distortions in National Coordinates

A national map projection frame is not a 3-D Cartesian coordinate system, and its scale is commonly slightly different from that of a Cartesian frame defined in the WGS 84 datum [8]. Accordingly, if georeferencing is performed in national coordinates, the ground coordinates directly calculated from imaging sensor observations and exterior orientation parameters (EOPs) will not be located at correct positions [3], [9], [10]. According to [8], the errors originate from two sources, namely, the map projection distortion and the datum scale distortion, where the former can be further divided to three subcategories: one height distortion, two length distortions, and three angle distortions.

III. METHODS

A. Method of Zhao et al.

The attitude transformation method of Zhao *et al.* can be summarized as the following three steps [7].

1) Selecting three auxiliary points (APs) around the sensor center position. A recommended scheme of the AP positions given by Zhao *et al.* is

$$(\boldsymbol{T}^{\mathrm{s}}_{\mathrm{AP1}}, \boldsymbol{T}^{\mathrm{s}}_{\mathrm{AP2}}, \boldsymbol{T}^{\mathrm{s}}_{\mathrm{AP3}}) = \begin{pmatrix} 0.1 & 0 & 0 \\ 0 & 0.1 & 0 \\ 0 & 0 & 0.1 \end{pmatrix} \tag{1}$$

where $\boldsymbol{T}^{\mathrm{s}}_{\mathrm{AP}}$ is the auxiliary vector (i.e., the column vector parameterized by the 3-D coordinate of an AP) in the s-frame, and the coordinate unit is in meters.
2) Transforming these three APs and the sensor center into the p-frame. As schematically shown in Fig. 1, the transformation workflow of an AP from the s-frame to the p-frame is slightly complicated than that of the sensor center (i.e., the GPS/INS position transformation process). The latter actually can be seen as a special case of the former, i.e., when $\boldsymbol{T}^{\mathrm{s}}_{\mathrm{AP}} = \begin{pmatrix} 0 & 0 & 0 \end{pmatrix}^{\mathrm{T}}$.
3) Calculating the attitude matrix $\boldsymbol{R}^{\mathrm{p}}_{\mathrm{s}}$ from

$$\begin{aligned}&(\boldsymbol{T}^{\mathrm{p}}_{\mathrm{AP1}} - \boldsymbol{T}^{\mathrm{p}}_{\mathrm{S}}, \boldsymbol{T}^{\mathrm{p}}_{\mathrm{AP2}} - \boldsymbol{T}^{\mathrm{p}}_{\mathrm{S}}, \boldsymbol{T}^{\mathrm{p}}_{\mathrm{AP3}} - \boldsymbol{T}^{\mathrm{p}}_{\mathrm{S}}) \\ &\quad = \boldsymbol{R}^{\mathrm{p}}_{\mathrm{s}} \cdot (\boldsymbol{T}^{\mathrm{s}}_{\mathrm{AP1}} - \boldsymbol{T}^{\mathrm{s}}_{\mathrm{S}}, \boldsymbol{T}^{\mathrm{s}}_{\mathrm{AP2}} - \boldsymbol{T}^{\mathrm{s}}_{\mathrm{S}}, \boldsymbol{T}^{\mathrm{s}}_{\mathrm{AP3}} - \boldsymbol{T}^{\mathrm{s}}_{\mathrm{S}})\end{aligned} \tag{2}$$

where $\boldsymbol{T}^{\mathrm{s}}_{\mathrm{S}}$ and $\boldsymbol{T}^{\mathrm{p}}_{\mathrm{S}}$ refer to the column vectors parameterized by the 3-D coordinate of the sensor center S given in the s-frame and in the p-frame, respectively. Note that $\boldsymbol{T}^{\mathrm{s}}_{\mathrm{S}}$ is actually equal to $\begin{pmatrix} 0 & 0 & 0 \end{pmatrix}^{\mathrm{T}}$, and accordingly, $\boldsymbol{R}^{\mathrm{p}}_{\mathrm{s}}$ can be given by

$$\begin{aligned}\boldsymbol{R}^{\mathrm{p}}_{\mathrm{s}} = &(\boldsymbol{T}^{\mathrm{p}}_{\mathrm{AP1}} - \boldsymbol{T}^{\mathrm{p}}_{\mathrm{S}}, \boldsymbol{T}^{\mathrm{p}}_{\mathrm{AP2}} - \boldsymbol{T}^{\mathrm{p}}_{\mathrm{S}}, \boldsymbol{T}^{\mathrm{p}}_{\mathrm{AP3}} - \boldsymbol{T}^{\mathrm{p}}_{\mathrm{S}}) \\ &\cdot (\boldsymbol{T}^{\mathrm{s}}_{\mathrm{AP1}}, \boldsymbol{T}^{\mathrm{s}}_{\mathrm{AP2}}, \boldsymbol{T}^{\mathrm{s}}_{\mathrm{AP3}})^{-1}.\end{aligned} \tag{3}$$

If the angular EOPs (i.e., the three Euler angles) in the p-frame are needed, they can further be calculated from the matrix $\boldsymbol{R}^{\mathrm{p}}_{\mathrm{s}}$ [7].

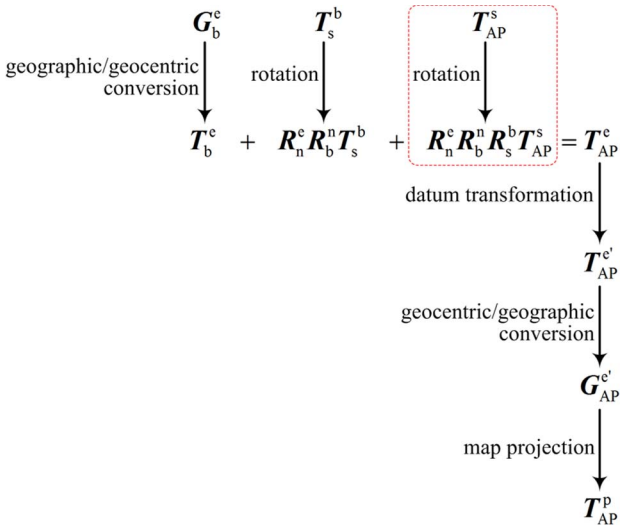

Fig. 1. Transformation process of an AP from the s-frame to the p-frame. The notation $\boldsymbol{T}$ represents the column vector constituted by the 3-D Cartesian coordinate (for the s-frame, b-frame, e-frame, or e′-frame) or the map projection coordinate (for the p-frame), and $\boldsymbol{G}$ refers to the geographic coordinate. The specific transformation formulas can be found in [3], [6], and [8].

B. Improved Method

The deficiency of the algorithm of Zhao *et al.* is that the mathematical form of (2) can be only applied for describing the rotation relationship between two Cartesian frames. Influenced by the map projection and the datum scale difference, the three auxiliary vectors in the p-frame are no longer orthogonal to each other, and their lengths are different from those in the s-frame, and accordingly, the improved solution is to offset the effect of the georeferencing distortions as much as possible. Given that the lengths of the auxiliary vectors are very short, only the datum scale distortion and the length distortion are numerically significant and therefore should be compensated. Accordingly, (3) is revised to

$$\begin{aligned}\boldsymbol{R}^{\mathrm{p}}_{\mathrm{s}} = &\begin{bmatrix} \frac{X^{\mathrm{p}}_{\mathrm{AP1}} - X^{\mathrm{p}}_{\mathrm{S}}}{k_{\mathrm{ld}} m} & \frac{X^{\mathrm{p}}_{\mathrm{AP2}} - X^{\mathrm{p}}_{\mathrm{S}}}{k_{\mathrm{ld}} m} & \frac{X^{\mathrm{p}}_{\mathrm{AP3}} - X^{\mathrm{p}}_{\mathrm{S}}}{k_{\mathrm{ld}} m} \\ \frac{Y^{\mathrm{p}}_{\mathrm{AP1}} - Y^{\mathrm{p}}_{\mathrm{S}}}{k_{\mathrm{ld}} m} & \frac{Y^{\mathrm{p}}_{\mathrm{AP2}} - Y^{\mathrm{p}}_{\mathrm{S}}}{k_{\mathrm{ld}} m} & \frac{Y^{\mathrm{p}}_{\mathrm{AP3}} - Y^{\mathrm{p}}_{\mathrm{S}}}{k_{\mathrm{ld}} m} \\ \frac{Z^{\mathrm{p}}_{\mathrm{AP1}} - Z^{\mathrm{p}}_{\mathrm{S}}}{m} & \frac{Z^{\mathrm{p}}_{\mathrm{AP2}} - Z^{\mathrm{p}}_{\mathrm{S}}}{m} & \frac{Z^{\mathrm{p}}_{\mathrm{AP3}} - Z^{\mathrm{p}}_{\mathrm{S}}}{m} \end{bmatrix} \\ &\cdot (\boldsymbol{T}^{\mathrm{s}}_{\mathrm{AP1}}, \boldsymbol{T}^{\mathrm{s}}_{\mathrm{AP2}}, \boldsymbol{T}^{\mathrm{s}}_{\mathrm{AP3}})^{-1}\end{aligned} \tag{4}$$

where X^{p} and Y^{p} refer to the east and north coordinates in the p-frame, respectively; Z^{p} is the ellipsoidal height; m is the

datum scale factor; and k_{ld} refers to the length distortion scale factor and can be given by [3]

$$k_{\mathrm{ld}} = \frac{kR}{R + Z_{\mathrm{S}}^{\mathrm{p}}} \tag{5}$$

where R is the mean radius of curvature at the sensor center and can be given by [11]

$$R = \frac{a\sqrt{1-e^2}}{1 - e^2 \sin^2 \varphi} \tag{6}$$

where a and e are the major radius and the first eccentricity of the national ellipsoid, respectively; and φ is the latitude of the sensor center.

The symbol k in (5) is the point scale factor. For the most widely used transverse Mercator projection, k can be given by [11]

$$k = k_0 \left(1 + \frac{X_{\mathrm{S}}^2}{2k_0^2 R^2} + \frac{X_{\mathrm{S}}^4}{24k_0^4 R^4}\right) \tag{7}$$

where X_{S} is the east coordinate of the sensor center in the p-frame without adding the false easting, and k_0 is the point scale factor at the central meridian. For the widely used Gauss–Krüger projection and universal transverse Mercator (UTM) projection, the values of k_0 are 1.0 and 0.9996, respectively.

IV. Experiments

A. Strategy

The accuracies of GPS/INS attitude transformation methods were evaluated by comparing the direct georeferencing (DG) results in the e-frame with those in the p-frame. First, DG was performed in the e-frame, and then, the ground points were transformed into the p-frame. Afterward, we converted POS data into the p-frame by using different attitude transformation methods and then performed DG with correcting georeferencing distortions. As a very high precision map projection algorithm [12] and a georeferencing distortion correction algorithm [8] were used in the experiment, we can safely conclude that almost all the disparities between the DG results in the e-frame and the p-frame were derived from the test attitude transformation methods.

Unlike previous studies that made use of field or simulated aerial imageries [3], [7], we employed simulated LiDAR data in our experiments. The advantage of our strategy is that the error propagation process and the residual analysis are much simpler, because the LiDAR DG process only relates to one sensor center, whereas the DG model of an aerial imagery involves multiple perspective centers.

B. Data

To fully evaluate the performance of different attitude transformation methods, both real and simulated POS data were used in our experiments. The field POS data were obtained from an airborne LiDAR project acquired by a Leica ALS50-II laser scanner. As schematically shown in Fig. 2, the survey

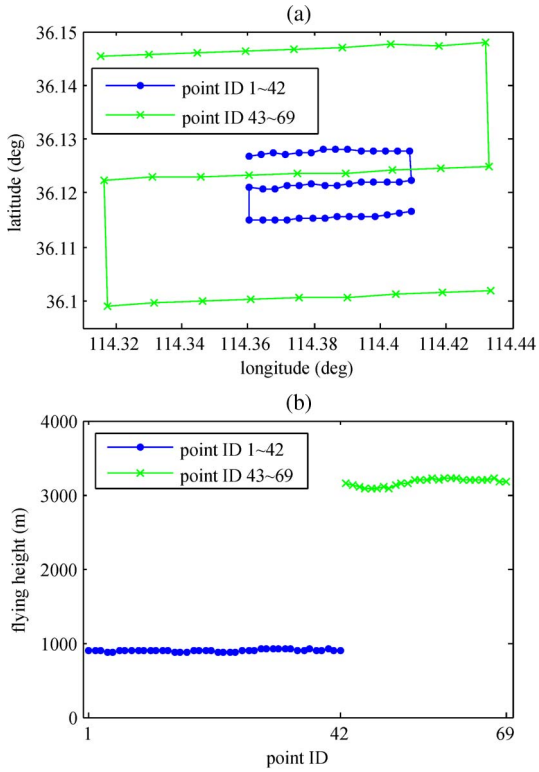

Fig. 2. Real POS data. (a) Planimetric and (b) altimetric coordinate distributions of perspective centers.

TABLE I
Technical Parameters of the Experimental National Map Projection Frame

Category	Parameter	Value
7-parameter w.r.t.	m	1.00005
WGS 84 datum	X	370.9492 m
	Y	282.6227 m
	Z	−4.7778 m
	α_ω	−0.0014°
	α_φ	0.0022°
	α_κ	−0.0025°
National ellipsoid	Type	Krassovsky
Map projection	Type	UTM
	Central meridian	117°

block includes six strips with a total of 69 images captured by the onboard medium-format camera. The flight heights of the first three and last three strips are about 900 and 3200 m, respectively; accordingly, the simulated LiDAR observation vectors were set to (−320 m, 160 m, −800 m) and (−1200 m, 600 m, −3000 m), respectively. The lever arms and boresight angles (i.e., the mounting parameters) were simulated to be (0.5 m, 0.03 m, −2.2 m) and (0.05°, −0.1°, 0.25°), respectively. The definition of the p-frame is shown in Table I.

Simulated GPS/INS data were also used in our experiments because they could better cover various survey scenarios. As shown in Table II, the data set includes 62 exposure stations, which are divided into six groups aiming to test the effects of position and attitude variations on the attitude transformation

TABLE II
SIMULATED POS DATA

Point ID	Variable [a]	Unit
1~13	$\lambda = [114:0.5:120]$ [b]	deg
14~22	$\varphi = [0:10:80]$	deg
23~31	$h = [0:1000:8000]$	m
32~40	$\alpha_r = [-8:2:8]$	deg
41~49	$\alpha_p = [-8:2:8]$	deg
50~62	$\alpha_h = [-180:30:180]$	deg

[a] The default values of the geographic coordinates and the attitude angles are $(\lambda, \varphi, h) = (120°\text{E}, 40°\text{N}, 8000\text{m})$ and $(\alpha_r, \alpha_p, \alpha_h) = (-2°, 4°, -90°)$, respectively; some of them were replaced with the variables which were calculated from the codes in the table.

[b] This is a pseudo Matlab code, which means that the longitude varies from 114° to 120° and the step is 0.5°.

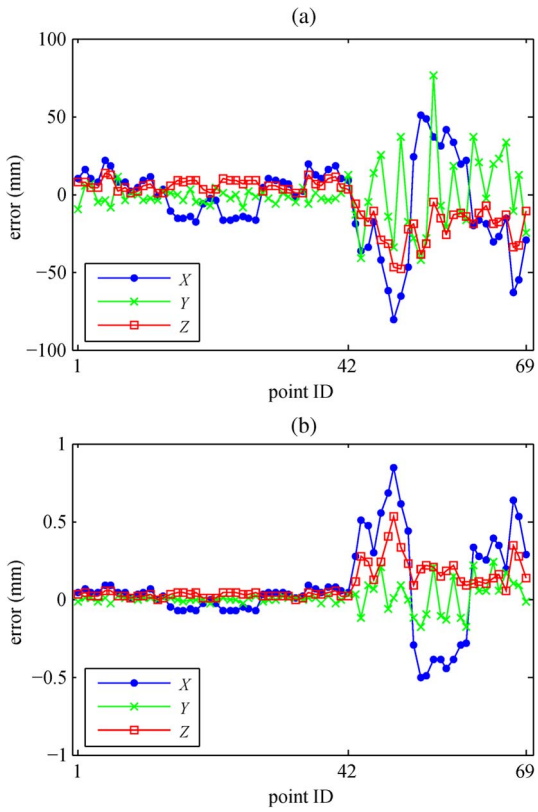

Fig. 3. Direct georeferencing errors in the real POS data experiment. Attitude data transformed by the (a) method of Zhao *et al.* and the (b) improved method. Two zones of point IDs represent the blocks with different flying heights [see Fig. 2(b)].

accuracies. The simulated LiDAR observation vector was set to (100 m, 500 m, −8000 m), and the mounting parameters and the p-frame definition were the same as those of the real POS data set.

C. Results

Figs. 3 and 4 depict the DG errors in the p-frame when different attitude transformation algorithms were used in the real and simulated POS data experiments, respectively. It is clearly shown that large DG errors occurred in the results of the method of Zhao *et al.*, which indicates the unsatisfied accuracy of the attitude data in the p-frame. In the real data experiment, the DG errors of the last three strips (point IDs 43–69) are much larger than those of the first threes strips (point IDs 1–42). However, it cannot prove that the attitude transformation results of the last three strips are worse because they correspond to higher flying heights and larger LiDAR observation vectors. On the other hand, the simulated experimental results show that the performance of the method of Zhao *et al.* and our improved method significantly varies with different geographic coordinates and attitude angles.

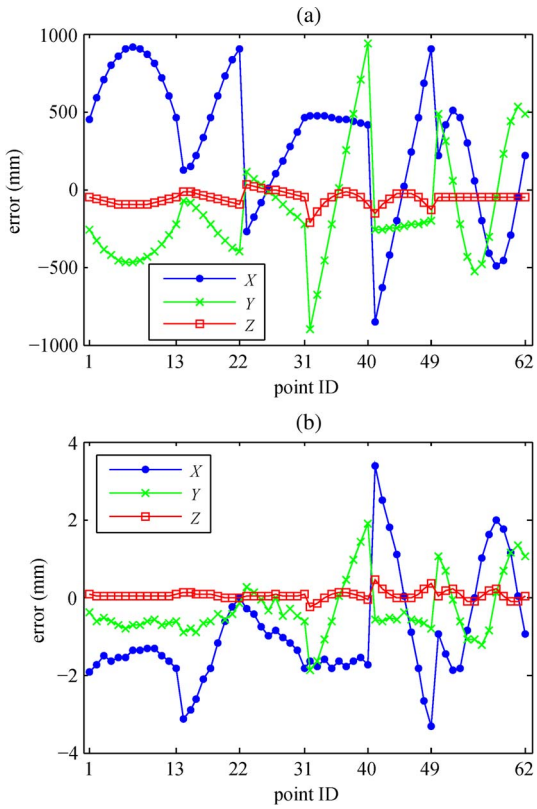

Fig. 4. Direct georeferencing errors in the simulated POS data experiment. Attitude data transformed by (a) the method of Zhao *et al.* and (b) the improved method. Six zones of point IDs represent different test variables [see Table II].

As the DG errors Δ_{DG} in the experiments are far smaller than the lengths of the LiDAR observation vectors $\boldsymbol{T}_{\text{DG}}$, we can use the following equation to approximately estimate the attitude transformation error:

$$\Delta_{\text{attitude}} = \frac{\|\Delta_{\text{DG}}\|}{\|\boldsymbol{T}_{\text{DG}}\|} \tag{8}$$

where Δ_{attitude} is in radians, and $\|\ \|$ is the Euclidean norm of a vector. The results show that the attitude transformation errors of the method of Zhao *et al.* are up to $1.8 \times 10^{-3^\circ}$ and $6.7 \times 10^{-3^\circ}$ in the real and simulated POS data experiments, respectively. Given that navigation grade or high-end tactical grade IMUs are typically integrated in state-of-the-art aerial imaging systems and their achievable accuracy can be as good as several 0.001° [13], [14], it can be concluded that the method

of Zhao *et al.* cannot meet the accuracy requirement of high-precision aerial photogrammetry. The maximum errors of our improved method in the real and simulated POS data experiments are $1.8 \times 10^{-5^\circ}$ and $2.5 \times 10^{-5^\circ}$, respectively, which can be safely ignored in practice because they are much smaller than most of the errors in the aerial photogrammetric data processing chain.

V. Conclusion

In this letter, we have presented an improved algorithm on the coordinate-transformation-based approach of Zhao *et al.* for transforming GPS/INS attitude data to the national map projection frame. Our experimental results demonstrate that the maximum error of the method of Zhao *et al.* can be up to several 0.001°. By correcting the datum scale distortion and the length distortion, our improved method can reduce the errors by two orders of magnitude, which is able to meet the requirement of high-precision aerial photogrammetry.

References

[1] M. Cramer *et al.*, "Data capture," *Handbook Geographic Information*, W. Kresse and D. M. Danko Eds. Berlin, Germany: Springer-Verlag, 2012, pp. 211–301.

[2] R. Sandau, *Digital Airborne Camera: Introduction and Technology*. Berlin, Germany: Springer-Verlag, 2010.

[3] K. Legat, "Approximate direct georeferencing in national coordinates," *ISPRS J. Photogramm. Remote Sens.*, vol. 60, no. 4, pp. 239–255, Jun. 2006.

[4] J. Skaloud and K. Legat, "Theory and reality of direct georeferencing in national coordinates," *ISPRS J. Photogramm. Remote Sens.*, vol. 63, no. 2, pp. 272–282, Mar. 2008.

[5] M. Bäumker and F. J. Heimes, "New calibration and computing method for direct georeferencing of image and scanner data using the position and angular data of an hybrid inertial navigation system," *Proc. OEEPE Workshop Integr. Sens. Orientation*, Hanover, Germany, 2002, 1–17.

[6] International Association of Oil & Gas Producers, 2014. Coordinate conversions and transformations including formulas. [Online] Available: http://www.ogp.org.uk/pubs/373-07-2.pdf

[7] H. Zhao, B. Zhang, C. Wu, Z. Zuo, and Z. Chen, "Development of a coordinate transformation method for direct georeferencing in map projection frames," *ISPRS J. Photogramm. Remote Sens.*, vol. 77, pp. 94–103, Mar. 2013.

[8] Y. Zhang and X. Shen, "Direct georeferencing of airborne LiDAR data in national coordinates," *ISPRS J. Photogramm. Remote Sens.*, vol. 84, pp. 43–51, Oct. 2013.

[9] Y. Zhang and X. Shen, "Approximate correction of length distortion for direct georeferencing in map projection frame," *IEEE Geosci. Remote Sens. Lett.*, vol. 10, no. 6, pp. 1419–1423, Nov. 2013.

[10] N. Yastikli and K. Jacobsen, "Direct sensor orientation for large scale mapping—Potential, problems, solutions," *Photogramm. Rec.*, vol. 20, no. 111, pp. 274–284, Sep. 2005.

[11] G. Bomford, *Geodesy*, 4th ed. Oxford, U.K.: Clarendon, 1980.

[12] C. F. F. Karney, GeographicLib, 2014. [Online] Available: http://geographiclib.sourceforge.net/

[13] Applanix. POS AV specifications, 2012. [Online] Available: http://www.applanix.com/media/downloads/products/specs/POSAV_SPECS.pdf

[14] J. Shan and C. K. Toth, *Topographic Laser Ranging and Scanning: Principles and Processing*. Boca Raton, FL, USA: CRC Press, 2008.